

Supporting Information

for

Intermediate-Volatility Organic Compound Emissions from On-road Diesel Vehicles: Chemical Composition, Emission Factors and Estimated Secondary Organic Aerosol Production

Yunliang Zhao^{1,2}, Ngoc T. Nguyen^{1,2}, Albert A. Presto^{1,2},

Christopher J. Hennigan^{1,2,3}, Andrew A. May^{1,2,4}, Allen L. Robinson^{*,1,2}

¹Center for Atmospheric Particle Studies, Carnegie Mellon University, 5000 Forbes Avenue, Pittsburgh, Pennsylvania 15213, United States

²Department of Mechanical Engineering, Carnegie Mellon University, 5000 Forbes Avenue, Pittsburgh, Pennsylvania 15213, United States

³now at: Department of Chemical, Biochemical and Environmental Engineering at the University of Maryland, Baltimore County, Maryland, 21250, United States

⁴now at: Department of Civil, Environmental, and Geodetic Engineering, The Ohio State University, Columbus, Ohio, United States

**E-mail:* alr@andrew.cmu.edu

This supporting information includes:

- S1. IVOC Background
- S2. Estimating SOA production from vehicle exhaust
- S3. Exhaust versus fuel composition
- S4. Figures (8) and Tables (9)

S1. IVOC background

The background IVOCs were measured by collecting adsorbent tubes during dynamic blank experiments when the CVS was operated only on clean air (no vehicle exhaust). Because of the dynamic processes of desorption and adsorption of IVOCs on the walls of the CVS tunnel,¹ these dynamic blanks may overestimate the amount of background IVOCs during an actual emission tests. However, the IVOC mass of dynamic blanks can indicate the interference of background IVOCs on emission measurements of IVOCs. The mass of IVOCs in dynamic blanks was less than 5% of IVOCs collected over all tests for vehicles without a diesel particulate filter (nonaftertreatment vehicles) and over the creep+idle cycle for DPF-equipped vehicles. However, the mass of IVOCs in dynamic blanks corresponded to a larger fraction of IVOCs during other tests of vehicles equipped a DPF, up to 42% of IVOCs collected during the UDDS cycle for the DPF- and SCR-equipped heavy duty diesel vehicle.

S2. Estimating SOA production from vehicle exhaust

The SOA production from IVOCs (speciated IVOCs and the UCM) and single-ring aromatic compounds was estimated using the approach of Zhao et al.² Briefly, SOA precursors are assumed to react with hydroxyl radical to produce semivolatile products. The product distribution for each precursor is taken from the literature; they are based on published fits of SOA production measured in single compound smog chamber experiments. The SOA yield is determined by the gas-particle partitioning of these semivolatile products calculated using absorptive partitioning theory assuming a quasi-ideal solution and measured

organic aerosol concentrations. The SOA yields and OH reaction rates used in the model are compiled in Table S7 - S9.

For speciated IVOCs and single-ring aromatics, the OH reaction rate constants are taken from either previous studies³⁻⁹ or calculated using structure-reactivity relationships.¹⁰ The SOA mass yields of these species are from published results of high-NOx chamber experiments with individual compounds.^{4, 11, 12} These data are compiled in Table S7.

The SOA production from the UCM is estimated by assigning surrogate compounds to unspciated *b*-alkanes and unspciated cyclic compounds in each of 11 retention-time bins. These surrogate compounds (*n*-alkanes) represent the SOA yields and OH reaction rates of the unspciated *b*-alkanes and unspciated cyclic compounds in each IVOC bin (Table S9).² These surrogate compounds were selected to account for the impacts of molecular structure and vapor pressures on SOA yields and OH reaction rates.^{2, 10, 13} The SOA mass yields of unspciated *b*-alkanes in the B_n bin are represented by the C_{n-2} *n*-alkane; the SOA mass yields of the unspciated cyclic compounds in the B_n bin are represented by the C_n *n*-alkane.² The SOA yields of *n*-alkanes are from the chamber experiments in Presto et al.¹² conducted at atmospheric relevant OA concentrations (Table S7). The OH reaction rate constants of both unspciated *b*-alkanes and cyclic compounds in the B_n bin are represented by the C_n *n*-alkane.

S3. Exhaust versus fuel composition

Previous studies have used unburned diesel fuel as a surrogate to estimate SOA production from diesel engine exhaust.¹⁴ However, both SOA yields and OH reaction rates depend on chemical composition;^{4, 10, 13} therefore this approach assumes that exhaust and diesel fuel have similar composition. The data collected here indicate both enrichment and depletion in IVOCs is found in exhaust compared to diesel fuel. The effects of these differences on SOA production are not known given that such a large fraction of the IVOC emissions cannot be speciated. However, they underscore the importance of characterizing the chemical composition of the actual emissions for estimating SOA production from diesel vehicles.

To investigate the similarity in the chemical composition, both exhaust and diesel fuel were analyzed by GC/MS. Total PAHs in the IVOC range are enriched in exhaust compared to diesel fuel. For example, the mass fractions of PAHs are 0.8%, 1.4% and 5.1% in tailpipe emissions with low-, mid- and high-aromatic diesel fuel; however, they are 0.4%, 0.7% and 4.7% in diesel fuel, respectively. The enrichment is greater in exhaust when vehicles were tested with relative low aromatic content diesel fuel (9% and 12%).

In contrast to PAHs, the *n*-alkanes are depleted in exhaust relative to diesel fuel. Figure S6 compares the mass fraction of *n*-alkanes in exhaust and diesel fuel.

The mass fractions of total *n*-alkanes to total IVOCs are substantially lower in the exhaust compared to diesel fuel across all tests, except for one *n*-alkane (tridecane) in the creep+idle test with low aromatic-content fuel shown in Figure S6a.

There are also differences in the IVOC UCM distribution between exhaust and diesel fuel. The IVOC UCM distribution (B12-B22) can be predicted using the mass fraction distribution of *n*-alkanes to total *n*-alkanes (C12-C22) given that a strong correlation exists between them ($R^2=0.8$, Figure S7). Figure S8 compares the mass fractions of *n*-alkanes to total alkanes in exhaust to diesel fuel. Both higher and lower mass fractions of *n*-alkanes to total *n*-alkanes in exhaust compared to diesel fuel are observed. The mass fractions of *n*-alkanes to total alkanes are depleted in the exhaust relative to diesel fuel for those with carbon number greater than 16. The mass fraction of the IVOC UCM to total IVOCs in diesel exhaust is expected to have the similar distribution as the *n*-alkanes and therefore is depleted at larger carbon numbers. The SOA yield is higher for the IVOC bin with larger bin number due to their lower volatility.^{12, 13} Therefore, the differences in the mass fraction distribution of the IVOC UCM to total IVOCs between exhaust and diesel fuels imply that using diesel fuel as the surrogate for exhaust likely overestimates SOA production from diesel exhaust.

S4. Figures and Tables

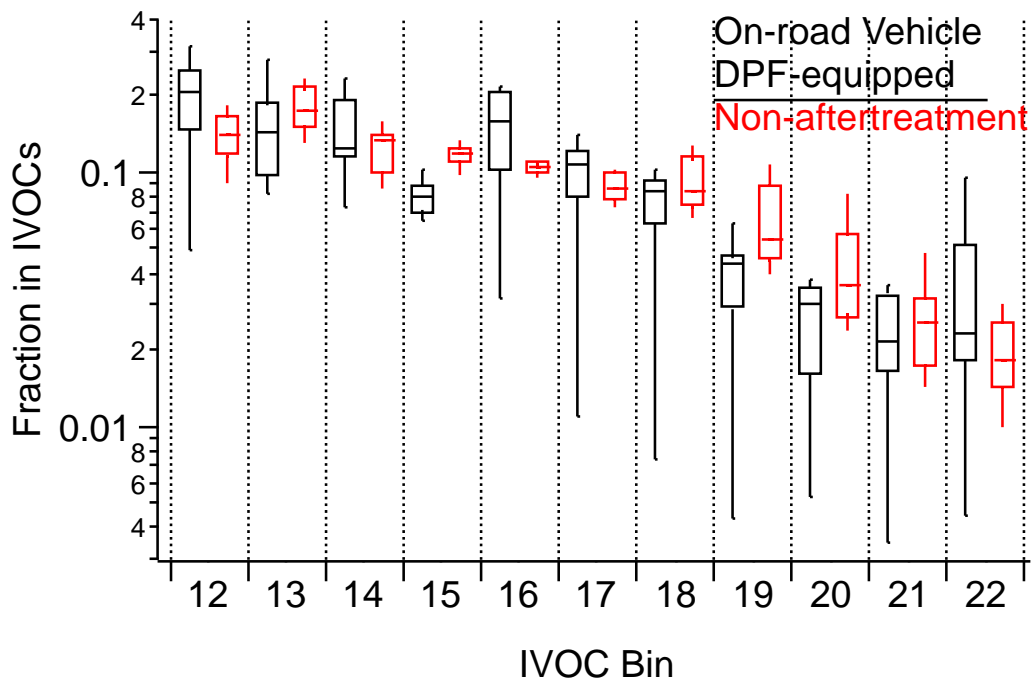


Figure S1. Volatility distributions of tailpipe IVOCs from DPF-equipped and nonaftertreatment diesel vehicles; data are plotted as mass fraction of total IVOCs.

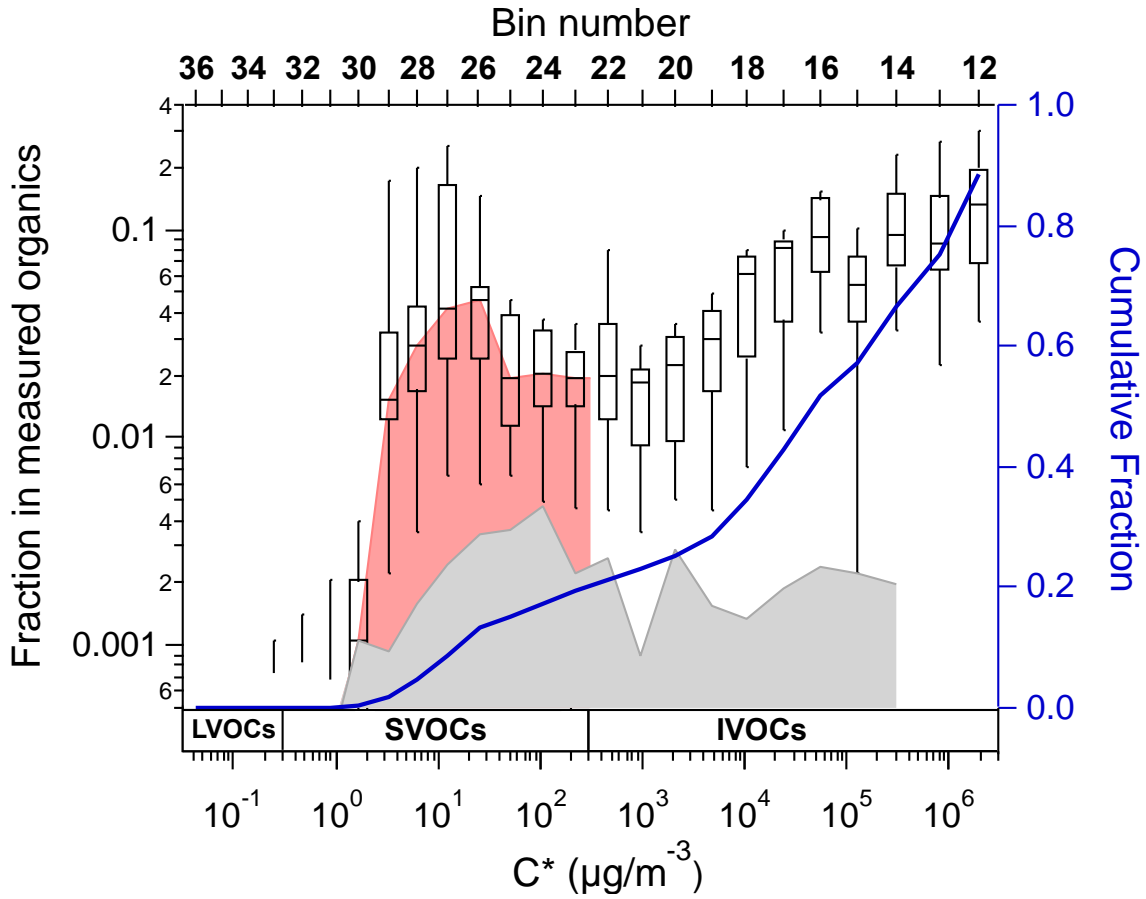


Figure S2. Mass fraction distributions of organics thermally desorbed during GC/MS analysis from the quartz filter/adsorbent tube sample sets collected from all of the DPF-equipped diesel tests. The boxes represent the 75th and 25th percentiles with the centerline being the median. The whiskers are the 90th and 10th percentiles. The grey area represents the median mass fraction of organics desorbed from quartz filters. The red area indicates the median SVOC breakthrough from the quartz filters.

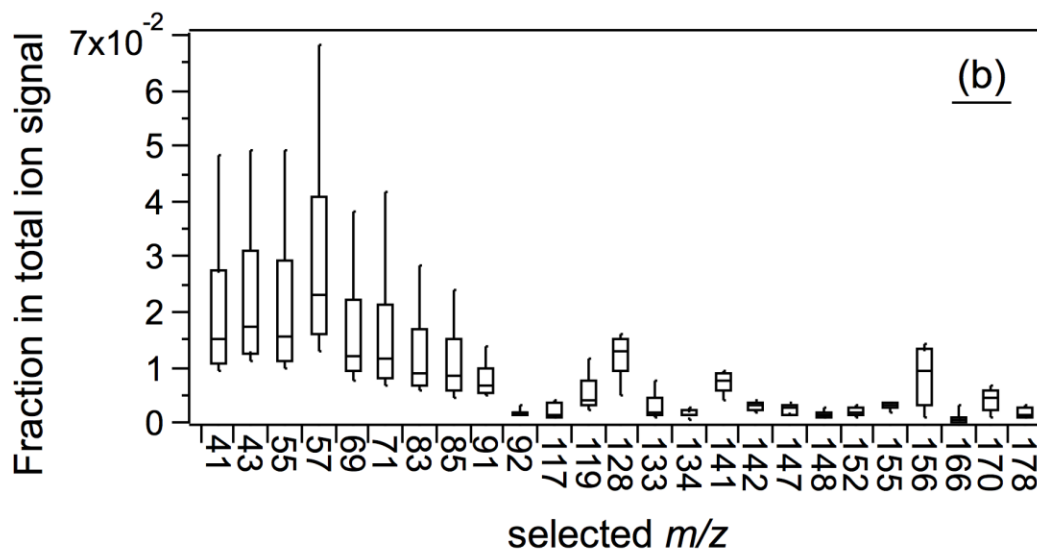
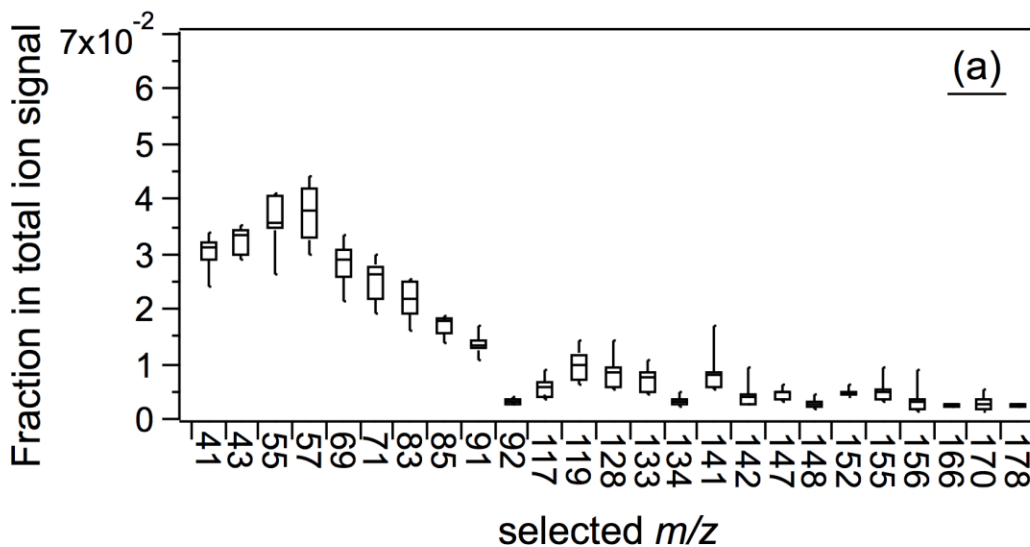


Figure S3. Selected mass fragments (m/z) measured during GC/MS analysis of a) adsorbent tubes collected from the entire set of tests with nonaftertreatment diesel vehicles and b) adsorbent tubes collected from the tests with DPF-equipped vehicles. The boxes represent the 75th and 25th percentiles with the centerline being the median. The whiskers are the 90th and 10th percentiles

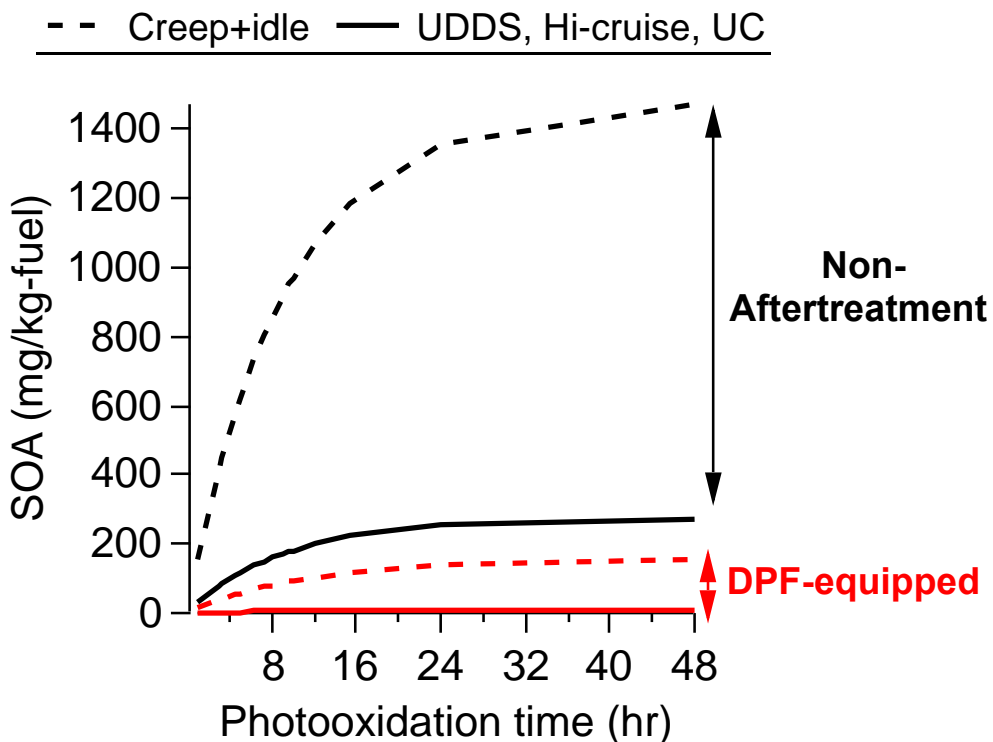


Figure S4. Predicted average SOA production from four categories of tests grouped by aftertreatment devices and drive cycle. The predictions are plotted as a function of photo-oxidation time assuming $[\text{OH}] = 1.5\text{E}+6$ molecules cm^{-3} .

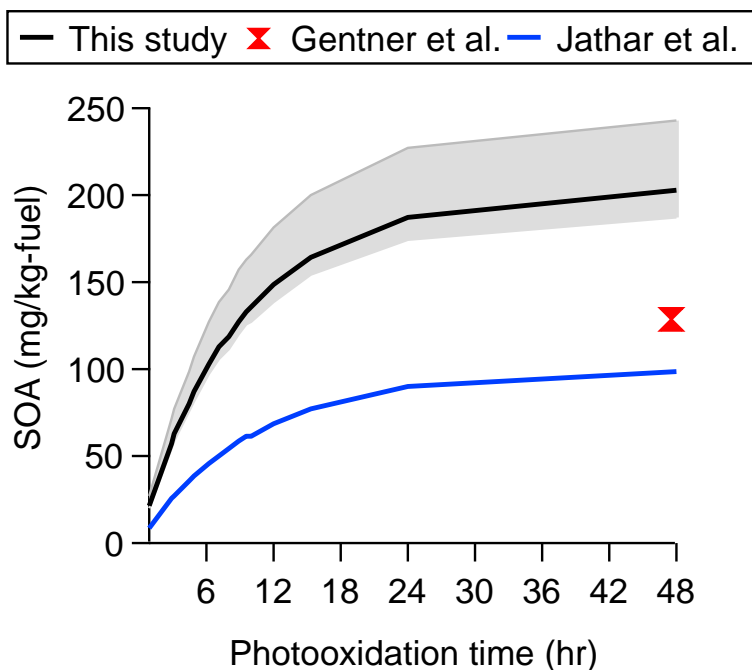


Figure S5 Comparison between our estimate of SOA from IVOCs and estimates in previous studies. The SOA production was plotted as a function of photooxidation time assuming $[OH]=1.5E+6$ molecules cm^{-3} . The estimated SOA production was made at the OA concentration of $10 \mu g /m^3$.

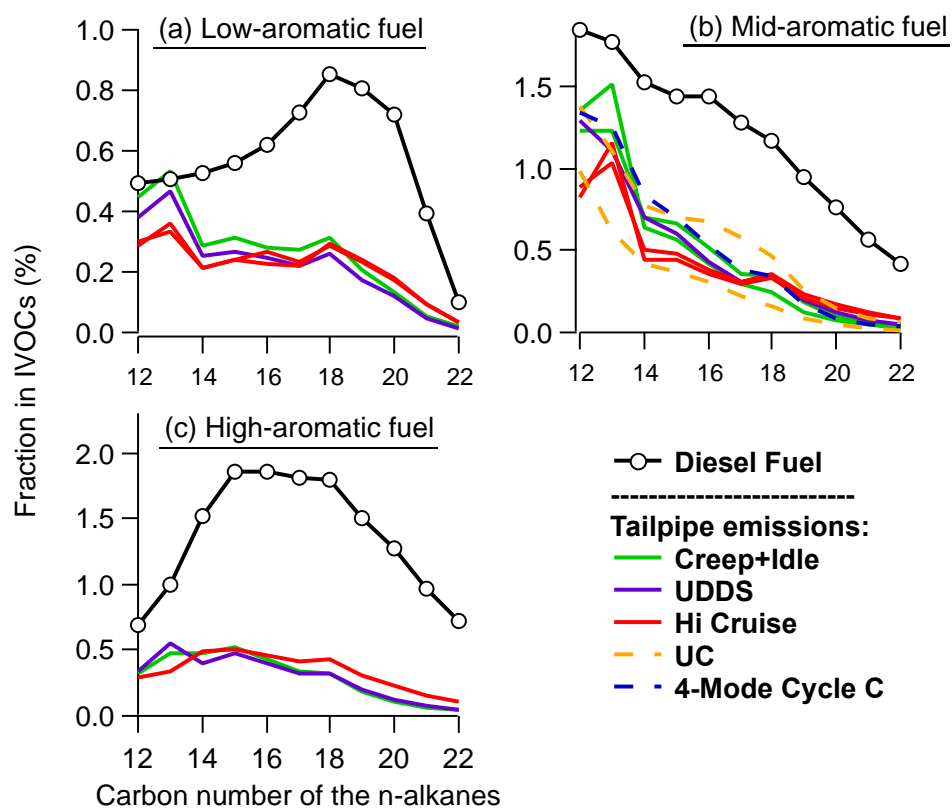


Figure S6. Comparison of *n*-alkanes distributions in tailpipe emissions and diesel fuels. Results are presented as mass fractions of total IVOCs.

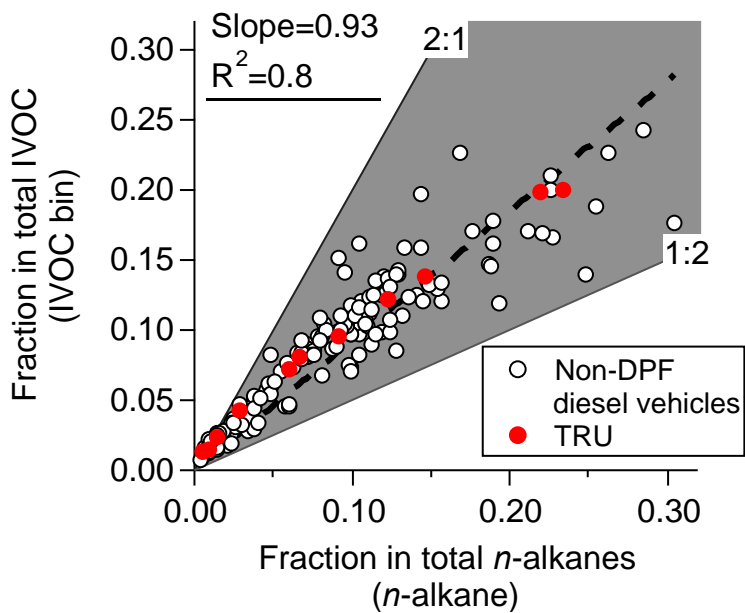


Figure S7. The correlation between the mass fraction of each IVOC UCM bin (B_n , $n=12\text{--}22$) bin to total IVOCs and the mass fraction of the *n*-alkane (C_n) to total *n*-alkanes. The data are for all nonaftertreatment vehicle tests.

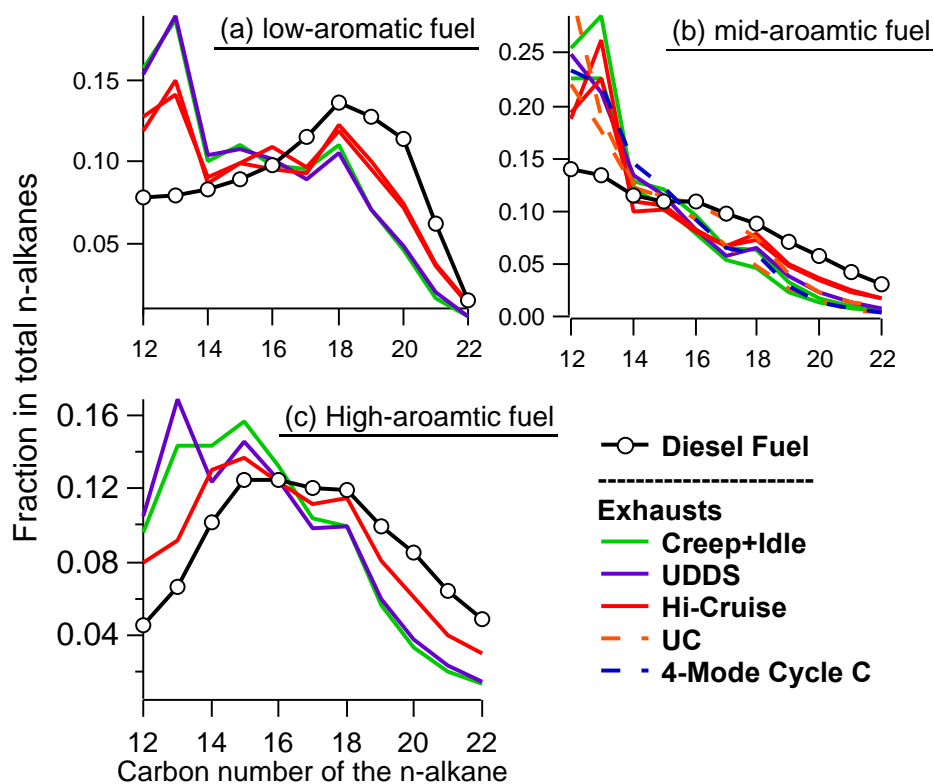


Figure S8. Comparison of mass fraction distribution of C12-C22 *n*-alkanes in the sum of these *n*-alkanes for emissions and diesel fuel.

Tables:

Table S1. Tested Diesel Engines.

<i>Vehicle ID</i>	<i>Model Year</i>	<i>Mileage</i>	<i>Aftertreatment Device</i>	<i>Engine Displacement (L)</i>	<i>Average Fuel economy (mpg)</i>
<i>On-road engine</i>					
1	2010	11000	DPF+SCR+DOC	14.9	4.5
2	2007	22000	DPF+DOC	12.8	4.9
3	2006	94000	none	10.8	4.3
4	2005	66000	DOC*	6.6	11.8
5	2001	159000	none	5.9	13.7
<i>Off-road engine</i>					
TRU	1998	>1000hrs	none	2.2	

Note: DOC: Diesel Oxidation Catalyst; DPF: Diesel Particulate Filter; SCR: Selective Catalytic Reduction. "*" indicates that the DOC is compromised.

Table S2. The driving schedule, fuel type, and measured fuel economy for each IVOC sample.

<i>Vehicle#</i>	<i>Test ID^a</i>	<i>Driving Cycle^b</i>	<i>Fuel type^c</i>	<i>FUEL ECONOMY (MPG)</i>
1	1450	3xCreep+ Idle	28% A	0.8
1	1458, 1461	4xUDDS	9% A	4.5
2	1419, 1920	6xCreep+ Idle	12% A	1.1
2	1413, 1415, 1417	6xUDDS	12% A	5.0
2	1418	2xUDDS	12% A	4.9
2	1406	2xUDDS	28% A	5.0
2	1411	2xUDDS	28% A	4.8
2	1421, 1422,1423	Cold start 6xUDDS	12% A	4.9
3	1443	3xCreep+ Idle	9% A	0.8
3	1445	2xUDDS	9% A	5.1
3	1444	3xHi-Cruise	9% A	7.7
3	1444	3xHi-Cruise	9% A	7.7
3	1434	3xCreep+ Idle	12% A	0.8
3	1436	3xCreep+ Idle	12% A	0.9
3	1433	2xUDDS	12%A	5.0
3	1435	3xHi-Cruise	12% A	7.6
3	1437	3xHi-Cruise	12% A	7.6
3	1439	3xCreep+ Idle	28% A	0.8
3	1441	2xUDDS	28% A	5.0
3	1440	3xHi-Cruise	28% A	7.5
4	1028019	Cold UC	12% A	11.7
5	1028080	Cold UC	12% A	14.4
TRU	1032421, 1032422	4-Mode Cycle C	12% A	n/a

Note: a) Each row represents one IVOC sample. For DPF-equipped vehicles (1 and 2), some samples were composites collected over multiple tests (indicated by the number of the test ID in each sample) to ensure sufficient IVOC loadings. The collection of IVOCs was conducted for the entire duration of each HDDV experiment. For MDDV experiments, IVOCs were collected during all three UC bags but not during the hot soak.

b) For HDDVs, each driving schedule was repeated multiple times consecutively during each test to increase IVOC loadings, such as two times for the UDDS (2xUDDS), three times for the cruise (3xhi-cruise) and three times for the creep followed by a period of engine idling (3xcreep+idle).

c) The fuel types are differentiated by their aromatic contents. For example, 28% A stands for 28% of the diesel fuel being aromatic compounds.

Table S3. Emission factors ($\mu\text{g}/\text{kg}\text{-fuel}$) of speciated IVOCs. (see the spreadsheet).

Table S4. Emission factors ($\text{mg}/\text{kg}\text{-fuel}$) of the IVOC UCM: unspciated *b*-alkanes and unspciated cyclic compounds. (see the spreadsheet).

Figure S4a. Emission factors ($\text{mg}/\text{kg}\text{-fuel}$) of unspciated *b*-alkanes and unspciated cyclic compounds presented in 11 bins (B12~B22) and emission factors ($\text{mg}/\text{kg}\text{-fuel}$) of total IVOCs, NMHCs and POA.

Figure S4b. Unspciated IVOC and total IVOC emission factors ($\text{mg}/\text{kg}\text{-fuel}$) presented in 4 ($C^*=10^3, 10^4, 10^5, 10^6 \mu\text{g}/\text{m}^3$ at 298°C) bins lumped based on the volatility basis set framework.

Table S5. The mass fraction distribution of total organics measured by GC/MS analysis of the quartz filter/adsorbent tube sample sets (the sum of IVOCs, SVOCs and LVOCs) described by their percentiles (10th, 50th and 90th) as a function of the effective saturation concentration (C^* , $\mu\text{g m}^{-3}$) at 298°C.

Table S5a. The mass fraction distribution of total measured organics by GC from nonaftertreatment diesel vehicles:

$\text{Log}(C^*)$	10 th	50 th	90 th
-1	0.002	0.007	0.014
0	0.003	0.009	0.014
1	0.015	0.026	0.044
2	0.016	0.025	0.043
3	0.049	0.081	0.129
4	0.170	0.207	0.300
5	0.271	0.336	0.372
6	0.220	0.294	0.388

Table S5b. The mass fraction distribution of total measured organics by GC from DPF-equipped diesel vehicles:

$\text{Log}(C^*)$	10 th	50 th	90 th
-1	0.000	0.001	0.002
0	0.000	0.002	0.006
1	0.018	0.114	0.627
2	0.016	0.058	0.113
3	0.013	0.068	0.128
4	0.023	0.180	0.211
5	0.119	0.281	0.361
6	0.085	0.214	0.569

Table S5c. The mass fraction distribution of total measured organics by GC and unrecovered OA in the VBS bin of $\text{Log}(C^*) < -1$ (only the 50th percentile) for nonaftertreatment diesel vehicles.

$\text{Log}(C^*)$	VBS2
<-1	0.034
-1	0.007
0	0.008
1	0.025
2	0.025
3	0.079
4	0.203
5	0.330
6	0.289

Table S6. Average mass fractions ($\mu\text{g}/\text{mg}$) of selected speciated IVOCs to total (speciated + unspeciated) IVOCs in the tailpipe emissions from nonaftertreatment diesel vehicles.

Compound	On-road diesel vehicles						TRU
	<i>low-aromatic fuel</i>		<i>mid-aromatic fuel</i>		<i>high-aromatic fuel</i>		<i>mid-aromatic fuel</i>
	<i>Ave</i>	<i>one stdev</i>	<i>Ave</i>	<i>one stdev</i>	<i>Ave</i>	<i>one stdev</i>	
<i>Dodecane</i>	3.54	0.73	11.37	2.30	3.19	0.22	13.42
<i>Tridecane</i>	4.24	0.92	11.08	2.67	4.55	1.04	12.58
<i>Tetradecane</i>	2.43	0.36	5.96	1.42	4.53	0.44	8.40
<i>Pentadecane</i>	2.65	0.36	5.47	1.21	4.99	0.22	7.05
<i>Hexadecaen</i>	2.56	0.22	4.40	1.24	4.35	0.28	5.25
<i>Heptadecane</i>	2.38	0.24	3.38	1.15	3.60	0.52	3.81
<i>Octadecane</i>	2.88	0.23	3.21	0.97	3.61	0.60	3.41
<i>Nonadecane</i>	2.13	0.29	1.87	0.59	2.28	0.63	1.67
<i>Eicosane</i>	1.52	0.30	1.18	0.45	1.54	0.63	0.84
<i>Heneicosane</i>	0.70	0.23	0.75	0.34	0.98	0.45	0.51
<i>Docosane</i>	0.26	0.10	0.51	0.26	0.69	0.38	0.33
<i>Pristane</i>	1.80	0.16	3.61	1.11	3.41	0.16	3.30
<i>Phytane</i>	1.30	0.08	2.35	0.87	2.82	0.46	1.84
<i>Naphthalene</i>	1.89	0.32	2.40	0.41	6.71	1.49	2.39
<i>Phenanthrene</i>	0.20	0.01	0.33	0.17	0.55	0.03	0.27

Table S7. OH reaction rate constants ($\text{cm}^3 \text{molec}^{-1} \text{s}^{-1}$) and SOA mass yields of speciated IVOCs.

Compound code	Compound name	OH rate constant	Yield at 10 $\mu\text{g}/\text{m}^3$ OA	Yield at 20 $\mu\text{g}/\text{m}^3$ OA
1	Dodecane	1.32E-11	0.09	0.12
2	Tridecane	1.51E-11	0.22	0.30
3	Tetradecane	1.68E-11	0.30	0.40
4	Pentadecane	1.82E-11	0.35	0.46
5	Hexadecaen	1.96E-11	0.40	0.51
6	Heptadecane	2.10E-11	0.44	0.55
7	Octadecane	2.24E-11	0.44	0.55
8	Nonadecane	2.38E-11	0.44	0.55
9	Eicosane	2.52E-11	0.44	0.55
10	Heneicosane	2.67E-11	0.44	0.55
11	Docosane	2.81E-11	0.44	0.55
12	2,6,10-Trimethylundecane	1.70E-11	0.04	0.07
13	2,6,10-Trimethyldodecane	1.87E-11	0.09	0.12
14	2,6,10-Trimethyltridecane	2.01E-11	0.22	0.30
15	2,6,10-Trimethylpentadecane	2.30E-11	0.35	0.46
16	Pristane	2.44E-11	0.35	0.46
17	Phytane	2.61E-11	0.40	0.51
18	Hexylcyclohexane	1.76E-11	0.09	0.12
19	Heptylcyclohexane	1.91E-11	0.22	0.30
20	Octylcyclohexane	2.05E-11	0.30	0.40
21	Nonylcyclohexane	2.19E-11	0.35	0.46
22	Decylcyclohexane	2.33E-11	0.40	0.51
23	Undecylcyclohexane	2.47E-11	0.44	0.55
24	Dodecylcyclohexane	2.61E-11	0.44	0.55
25	Tridecylcyclohexane	2.75E-11	0.44	0.55
26	Tetradecylcyclohexane	2.89E-11	0.44	0.55
27	Pentadecylcyclohexane	3.04E-11	0.44	0.55
28	Hexadecylcyclohexane	3.18E-11	0.44	0.55
29	Heptadecylcyclohexane	3.32E-11	0.44	0.55
30	Naphthalene	2.30E-11	0.22	0.27
31	2-methylnaphthalene	4.86E-11	0.31	0.40
32	1-methylnaphthalene	4.09E-11	0.26	0.34
33	C2-naphthalene	6.00E-11	0.31	0.31
34	C3-naphthalene	8.00E-11	0.31	0.31
35	C4-naphthalene	8.00E-11	0.31	0.31
36	Acenaphthylene	1.24E-10	0.31	0.31

Compound code	Compound name	OH rate constant	Yield at 10 $\mu\text{g}/\text{m}^3$ OA	Yield at 20 $\mu\text{g}/\text{m}^3$ OA
37	Acenaphthene	8.00E-11	0.31	0.31
38	Fluorene	1.60E-11	0.31	0.31
39	C1-Fluorene	8.00E-11	0.31	0.31
40	Phenanthrene	3.20E-11	0.31	0.31
41	Anthracene	1.78E-10	0.31	0.31
42	C1-Phenanthrene/Anthracene	5.89E-11	0.31	0.31
43	C2-Phenanthrene/Anthracene	8.00E-11	0.31	0.31
44	Fluoranthene	3.30E-11	0.31	0.31
45	Pyrene	5.60E-11	0.31	0.31
46	C1-Fluoranthene/Pyrene	1.31E-10	0.31	0.31
47	Pentylbenzene	1.01E-11	0.04	0.07
48	Hexylbenzene	1.15E-11	0.09	0.12
49	Heptylbenzene	1.30E-11	0.22	0.30
50	Octylbenzene	1.44E-11	0.30	0.40
51	Nonylbenzene	1.58E-11	0.35	0.46
52	Decylbenzene	1.72E-11	0.40	0.51
53	Undecylbenzene	1.86E-11	0.44	0.55
54	Dodecylbenzene	2.00E-11	0.44	0.55
55	Tridecylbenzene	2.14E-11	0.44	0.55
56	Tetradecylbenzene	2.29E-11	0.44	0.55
57	Pentadecylbenzene	2.43E-11	0.44	0.55

Note: 1) Data sources of OH rate constants: Compound#1, 2, 30 from Atkinson and Arey³; Compound #3-29 and 46-57 are calculated using the structure-reactivity relationships^{10,15}; Compound#31-35, 39, 43 are from Chan et al.⁴; Compound #36, 37 are from Reisen and Arey⁸; Compound #38 is from Kwok et al.⁶; Compound #40 and 42 are from Lee et al.⁷; Compound #41 is from Ananthula et al.⁹ and Compound#43, 44 are from Kameda et al.⁵

2) Data sources for SOA mass yields: Compound#1-6 are from Presto et al.¹²; Compound#7-11 are assumed to be the same as the compound #6 to provide conservative estimates; Compound #12-29 are derived based on the approach of Zhao et al.²; Compound#30-46 are from Chan et al.⁴; Compound#47-57 are assumed to be the same as *n*-alkanes with the same carbon number.

3) Calibration of GC/MS: Compound #1-11, 16, 17, 19-23, 30-32, 36-38, 40,41, 44,45 are quantified using authentic standards. The rest of IVOC species are quantified using secondary standards, which have similar molecular structure and retention time to the compounds of interest.

Table S8. OH reaction rate constants ($\text{cm}^3 \text{ molec}^{-1} \text{ s}^{-1}$) and SOA mass yields of single-ring aromatic compounds at the OA concentration of $20 \mu\text{g}/\text{m}^3$.^{3, 4, 11}

	OH rate constant	Yield
benzene	1.22E-12	0.21
toluene	5.63E-12	0.11
ethylbenzene	7.00E-12	0.11
m-/p-xylene	1.87E-11	0.06
styrene	5.80E-11	0.11
o-xylene	1.36E-11	0.06

Table S9. OH reaction rate constants ($\text{cm}^3 \text{ molec}^{-1} \text{ s}^{-1}$) and surrogate compounds (*n*-alkanes) for SOA mass yields of unspciated IVOCs. Yield data for surrogate species (*n*-alkanes) are listed in Table S7.

Bin#	OH rate constant	Surrogate compounds (<i>n</i> -alkanes) for SOA yields	
		Unspciated <i>n</i> -alkanes	Unspciated cyclic compounds
B12	1.32E-11	C10	C12
B13	1.51E-11	C11	C13
B14	1.68E-11	C12	C14
B15	1.82E-11	C13	C15
B16	1.96E-11	C14	C16
B17	2.10E-11	C15	C17
B18	2.24E-11	C16	C18
B19	2.38E-11	C17	C19
B20	2.52E-11	C18	C20
B21	2.67E-11	C19	C21
B22	2.81E-11	C20	C22

References:

1. May, A. A.; Presto, A. A.; Hennigan, C. J.; Nguyen, N. T.; Gordon, T. D.; Robinson, A. L., Gas-Particle Partitioning of Primary Organic Aerosol Emissions: (2) Diesel Vehicles. *Environ. Sci. Technol.* **2013**, *47*, (15), 8288-8296.
2. Zhao, Y. L.; Hennigan, C. J.; May, A. A.; Tkacik, D. S.; de Gouw, J. A.; Gilman, J. B.; Kuster, W. C.; Borbon, A.; Robinson, A. L., Intermediate-Volatility Organic Compounds: A Large Source of Secondary Organic Aerosol. *Environ. Sci. Technol.* **2014**, *48*, (23), 13743-13750.
3. Atkinson, R.; Arey, J., Atmospheric degradation of volatile organic compounds. *Chem. Rev. (Washington, DC, U. S.)* **2003**, *103*, (12), 4605-4638.
4. Chan, A. W. H.; Kautzman, K. E.; Chhabra, P. S.; Surratt, J. D.; Chan, M. N.; Crouse, J. D.; Kurten, A.; Wennberg, P. O.; Flagan, R. C.; Seinfeld, J. H., Secondary organic aerosol formation from photooxidation of naphthalene and alkylnaphthalenes: implications for oxidation of intermediate volatility organic compounds (IVOCs). *Atmos. Chem. Phys.* **2009**, *9*, (9), 3049-3060.
5. Kameda, T.; Inazu, K.; Asano, K.; Murota, M.; Takenaka, N.; Sadanaga, Y.; Hisamatsu, Y.; Bandow, H., Prediction of rate constants for the gas phase reactions of triphenylene with OH and NO₃ radicals using a relative rate method in CCl₄ liquid phase-system. *Chemosphere* **2013**, *90*, (2), 766-771.
6. Kwok, E. S. C.; Atkinson, R.; Arey, J., Kinetics of the gas-phase reactions of indan, indene, fluorene, and 9,10-dihydroanthracene with OH radicals, NO₃ radicals, and O₃ (vol 29, pg 299, 1997). *Int. J. Chem. Kinet.* **1997**, *29*, (8), 645-645.
7. Lee, W.; Stevens, P. S.; Hites, R. A., Rate constants for the gas-phase reactions of methylphenanthrenes with OH as a function of temperature. *J. Phys. Chem. A* **2003**, *107*, (34), 6603-6608.
8. Reisen, F.; Arey, J., Reactions of hydroxyl radicals and ozone with acenaphthene and acenaphthylene. *Environ. Sci. Technol.* **2002**, *36*, (20), 4302-4311.
9. Ananthula, R.; Yamada, T.; Taylor, P. H., Kinetics of OH radical reaction with anthracene and anthracene-d(10). *J. Phys. Chem. A* **2006**, *110*, (10), 3559-3566.
10. Kwok, E. S. C.; Atkinson, R., Estimation of Hydroxyl Radical Reaction-Rate Constants for Gas-Phase Organic-Compounds Using a Structure-Reactivity Relationship - an Update. *Atmos. Environ.* **1995**, *29*, (14), 1685-1695.
11. Ng, N. L.; Kroll, J. H.; Chan, A. W. H.; Chhabra, P. S.; Flagan, R. C.; Seinfeld, J. H., Secondary organic aerosol formation from m-xylene, toluene, and benzene. *Atmos. Chem. Phys.* **2007**, *7*, (14), 3909-3922.
12. Presto, A. A.; Miracolo, M. A.; Donahue, N. M.; Robinson, A. L., Secondary Organic Aerosol Formation from High-NO_x Photo-Oxidation of Low Volatility Precursors: n-Alkanes. *Environ. Sci. Technol.* **2010**, *44*, (6), 2029-2034.
13. Lim, Y. B.; Ziemann, P. J., Effects of Molecular Structure on Aerosol Yields from OH Radical-Initiated Reactions of Linear, Branched, and Cyclic Alkanes in the Presence of NO_x. *Environ. Sci. Technol.* **2009**, *43*, (7), 2328-2334.
14. Gentner, D. R.; Isaacman, G.; Worton, D. R.; Chan, A. W. H.; Dallmann, T. R.; Davis, L.; Liu, S.; Day, D. A.; Russell, L. M.; Wilson, K. R.; Weber, R.; Guha, A.; Harley, R. A.; Goldstein, A. H., Elucidating secondary organic aerosol from diesel and gasoline

vehicles through detailed characterization of organic carbon emissions. *Proc. Natl. Acad. Sci. U. S. A.* **2012**, *109*, (45), 18318-18323.

15. USEPA, Estimation Programs Interface Suite **2014**.